

Multifunctional polymer vesicles for ultrasensitive magnetic resonance imaging and drug delivery†

Tianbin Ren,^a Qiuming Liu,^a Hang Lu,^a Hongmei Liu,^{bc} Xin Zhang^{*b} and Jianzhong Du^{**a}

Received 27th March 2012, Accepted 23rd April 2012

DOI: 10.1039/c2jm31891a

Presented in this article is the synthesis of a new class of block copolymer, poly(ethylene oxide)-*block*-poly(*tert*-butyl acrylate-*stat*-acrylic acid) [PEO-*b*-P(AA-*stat*-*t*BA)], which can self-assemble into polymer vesicles with tuneable sizes at various conditions. The biocompatible and hydrophilic PEO chains form the vesicle coronas, while the PAA-*stat*-*t*BA chains form the membrane.

Superparamagnetic iron oxide nanoparticles (SPIONs) were generated *in situ* within the membrane of the polymer vesicles by nanoprecipitation. ¹H NMR, GPC, DLS, TGA, VSM and TEM were employed to characterize the structure and properties of the block copolymer, polymer vesicles and Fe₃O₄-decorated magnetic polymer vesicles. The water-dispersible, biocompatible, drug deliverable and superparamagnetic polymer vesicles exhibited excellent colloidal stability at a range of pH conditions and very high *T*₂ relaxivity, demonstrating ultra-sensitivity for magnetic resonance imaging and promising potential applications in nanomedicine.

Introduction

Cancer is one of the top ten leading causes of death in the world and it is estimated that 7.4 million people died of cancer in 2004. If current trends continue, 83.2 million more will have died by 2015.¹ Chemotherapy is one of the three main methods for cancer treatment.² In order to improve the accuracy of diagnosis/prognosis and to enhance the efficacy of cancer therapy, nanoparticles for simultaneous delivery of therapeutic and diagnostic agents were thought as one of the most promising ideas for treatment.^{3–5} A new term “theranostics” has been proposed, whereby it is defined as a combination of active and passive targeting, stimulus-responsive drug release, molecular imaging, and other therapeutic and diagnostic functions into a single platform.³ Usually, theranostic nanoparticles are multifunctional due to the co-incorporation of both therapeutic and imaging agents in one particle.

Magnetic resonance imaging (MRI) is one of the most powerful and non-invasive clinical imaging modalities with

high spatial resolution.⁶ The MRI sensitivity can be significantly enhanced in the presence of contrast agents.⁷ For application as either single nanoparticles or nanoparticle clusters, the particles must be highly magnetic,⁶ as well as also being biocompatible and fully dispersed in biological media without aggregation.⁸ The first human MRI study employed [Gd(DTPA)]²⁻ (DTPA = diethylenetriaminepentaacetic acid) complex as contrast agent.⁹ Metal nanoparticles such as gold nanorods have been incorporated with Gd as “multimodal” nanoparticles for MRI study because of desirable features of gold nanorods among nanoparticles, such as tunable absorption band, excellent stability and biocompatibility, *etc.*¹⁰ However, further study showed that the administration of high doses of these contrast agents led to concerns over accumulation and toxicity because of the extreme toxicity of free Gd(III).¹¹ Problems with slow excretion and toxicity due to long term accumulation may thus hinder future development of Gd(III) agents for superior contrast for tumour and vascular imaging.³ In contrast, superparamagnetic iron oxide nanoparticles with large surface area can prolong circulation time, improve stability and control over toxicity and targeting.¹² However, most of the contrast agents currently in use consist of low molecular weight compounds that are non-specific, and tend to aggregate due to strong magnetic dipole–dipole attractions between particles, combined with inherently large surface energy, making early diagnosis of diseases difficult.¹³ Therefore, multifunctional and hydrophilic polymeric nanocarriers are employed to prepare combined ultrasensitive superparamagnetic iron oxide nanoparticles to enhance the engineering specificity and sensitivity required for *in vivo* molecular imaging.⁶

^aSchool of Materials Science and Engineering, Research Centre for Advanced Materials, Key Laboratory of Advanced Civil Engineering Materials of Ministry of Education, Tongji University, 4800 Caoan Road, Shanghai, 201804, China. E-mail: jzdu@tongji.edu.cn; Fax: +86 021 6958 4723; Tel: +86 021 6958 0239

^bNational Key Laboratory of Biochemical Engineering, Institute of Process Engineering, Chinese Academy of Sciences, Beijing 100190, China. E-mail: xzhang@home.ipe.ac.cn

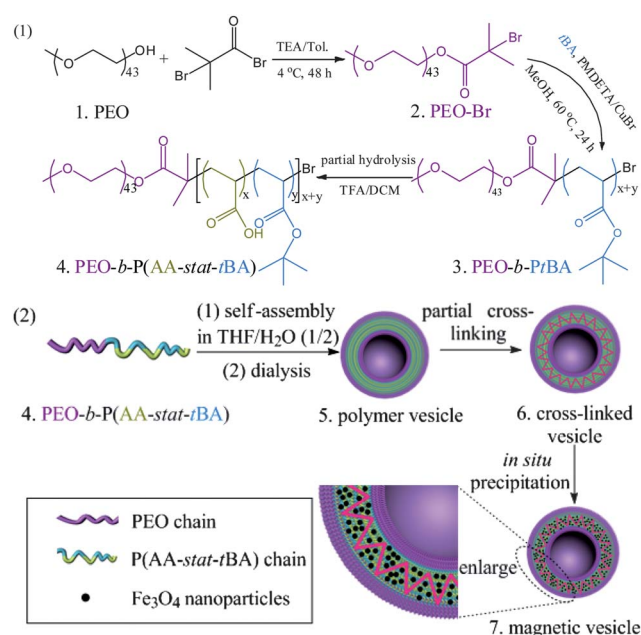
^cGraduate University of Chinese Academy of Sciences, Beijing 100049, China

† Electronic supplementary information (ESI) available: Fig. S1–S4: ¹H NMR spectrum, DLS correlation functions, TGA curves and magnetic hysteresis loop, as well as the calculation procedures for the copolymer composition. See DOI: 10.1039/c2jm31891a

Over the past decades various drug delivery and controlled release systems have been developed for cancer therapy. Polymer vesicles have been widely investigated because of their stable hollow structure and potential for advanced chemical functionalization and physiological applications.^{14–21} Usually, polymer vesicles are self-assembled from amphiphilic block copolymers, which have a hydrophobic, interdigitated or bilayer structure membrane, with hydrophilic coronas expressed inwards and outwards. They have been considered as an ideal drug delivery vehicle since both hydrophilic and hydrophobic drugs can be loaded either in the hydrophilic hollow cavity or the hydrophobic membrane in aqueous media. Recently, intelligent polymer vesicles¹⁵ have been developed which can respond to environmental stimuli such as a change in pH,^{22,23} temperature,^{24,25} light,²⁶ redox,²⁷ and electrical field,²⁸ *etc.*, to afford controlled release of encapsulated drugs.

Vesicular structures have been recently studied as clinical therapeutics and experimentally as diagnostic nanoparticles.^{29–32} For example, Lecommandoux and co-workers reported that hydrophobically modified maghemite ($\gamma\text{-Fe}_2\text{O}_3$) nanoparticles and an anticancer drug doxorubicin (DOX) were simultaneously encapsulated within the membrane of poly(trimethylene carbonate)-*b*-poly(L-glutamic acid) (PTMC-*b*-PGA) block copolymer vesicles.³³ Gong *et al.* prepared multifunctional spherical and worm-like polymer vesicles loaded with superparamagnetic iron oxide nanoparticles and DOX.^{34,35} However, in most cases, superparamagnetic nanoparticles are preformed and then loaded into the hollow cavity or the membrane of vesicles. In addition, improvements should be made for those particles to meet the requirements for clinical applications in diagnosis and therapy. Therefore, the preparation of water-dispersible and biocompatible magnetic vesicles with excellent colloidal stability, weak coalescence in strong magnetic field, and high magnetization still remains a challenge.

Herein, we present a new class of water-dispersible and biocompatible superparamagnetic polymer vesicles for MR imaging and anticancer drug delivery. Scheme 1 shows the synthetic route to the amphiphilic block-statistical copolymer and polymer vesicles decorated with superparamagnetic iron oxides in the vesicle membrane. (1) Amphiphilic block copolymer, poly(ethylene oxide)-*block*-poly(*tert*-butyl acrylate) (PEO-*b*-PtBA, polymer **1** in Table 1), is synthesized by atom-transfer radical polymerization (ATRP) with methoxy poly(ethylene oxide) bromide (PEO-Br) as the macro-initiator and *tert*-butyl acrylate (*t*BA) as the monomer. (2) Poly(ethylene oxide)-*block*-poly(*tert*-butyl acrylate-*stat*-acrylic acid) [PEO-*b*-P(AA-*stat*-*t*BA), Polymers **2**, **3** and **4** in Table 1] block-statistical copolymers are obtained by the partial hydrolysis of the PtBA in polymer **1** at various conditions. (3) Amphiphilic PEO-*b*-P(AA-*stat*-*t*BA) copolymer is dissolved in THF and then deionized water is added to induce vesicle formation. THF is then removed by subsequent dialysis against water. (4) The membrane of the vesicles is partially crosslinked by the reaction of PAA with the crosslinker, 2,2'-(ethylenedioxy)bis(ethylamine). (5) Superparamagnetic iron oxide nanoparticles (Fe_3O_4) were formed *in situ* in the membrane of the vesicles upon adding FeCl_3 and FeCl_2 solution by chemical nanoprecipitation. Those magnetic polymer vesicles can be utilized for theranostics in MR imaging and anticancer drug delivery.



Scheme 1 Synthetic route to water-dispersible, biocompatible and superparamagnetic polymer vesicles.

Results and discussion

Synthesis and characterization of PEO-*b*-P(AA-*stat*-*t*BA) block-statistical copolymers

PEO-*b*-P(AA-*stat*-*t*BA) block-statistical copolymers with various chain lengths were synthesized according to the following three steps illustrated in Scheme 1(1). (1) The PEO-Br macro-initiator was synthesized by esterification of MeO-PEO-OH with 2-bromoisobutryl bromide.¹⁶ The ¹H NMR analysis confirmed ~99% of esterification efficiency (Fig. S1, ESI†). (2) The PEO-*b*-PtBA diblock copolymer was synthesized by ATRP, using CuBr/PMDETA as catalyst system, PEO-Br as the macro-initiator and *tert*-butyl acrylate (*t*BA) as monomer. As shown in Fig. 1A, the peaks at 3.53 and at 2.20 ppm were assigned to $-\text{CH}_2-$ in PEO and $-\text{CH}-$ in the PtBA backbone, respectively. Gel permeation chromatographic (GPC) analysis of PEO₄₃-*b*-PtBA₆₅ diblock copolymer in Fig. 2 showed a low PDI of 1.16 and a significant increase in the molecular weight compared with PEO-Br macro-initiator. Therefore, both ¹H NMR analysis and GPC confirmed the successful synthesis of PEO₄₃-*b*-PtBA₆₅ diblock copolymer (Polymer **1**). (3) The PEO-*b*-P(AA-*stat*-*t*BA) block-statistical copolymers were synthesized by partial

Table 1 PEO-*b*-P(AA-*stat*-*t*BA) block-statistical copolymers by hydrolysis of PEO-*b*-PtBA diblock copolymer at various conditions

Polymer	Composition ^a	Ratio ^b	t_{hyd} ^c /min
1	PEO ₄₃ - <i>b</i> -PtBA ₆₅	—	—
2	PEO ₄₃ - <i>b</i> -P(AA ₉ - <i>stat</i> - <i>t</i> BA ₅₆)	1.5	10
3	PEO ₄₃ - <i>b</i> -P(AA ₂₅ - <i>stat</i> - <i>t</i> BA ₄₀)	3	15
4	PEO ₄₃ - <i>b</i> -P(AA ₅₀ - <i>stat</i> - <i>t</i> BA ₁₅)	5	60

^a The degree of polymerization (DP) of each block is determined by ¹H NMR; subscripts denote the DP of each monomer. ^b Molar ratio of TFA to *t*BA. ^c Hydrolysis time.

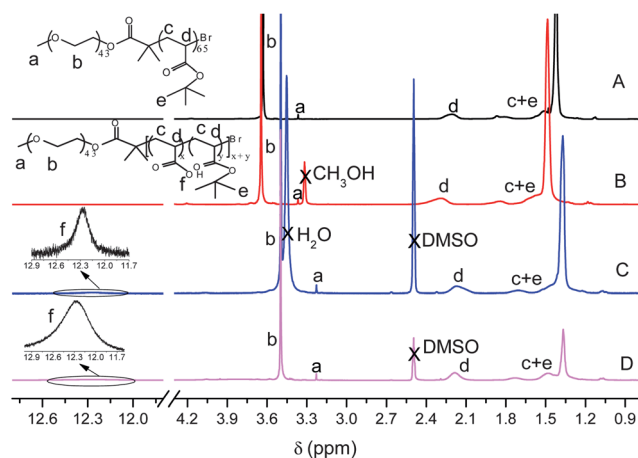


Fig. 1 ^1H NMR spectra of PEO-*b*-P(AA-*stat*-*t*BA) diblock copolymers with various degrees of hydrolysis: (A) PEO₄₃-*b*-PtBA₆₅ (polymer 1) in CDCl₃; (B) PEO₄₃-*b*-P(AA₉-*stat*-*t*BA₅₆) (polymer 2) in CH₃OH-*d*₄; (C) PEO₄₃-*b*-P(AA₂₅-*stat*-*t*BA₄₀) (polymer 3) in DMSO-*d*₆; (D) PEO₄₃-*b*-P(AA₅₀-*stat*-*t*BA₁₅) (polymer 4) in DMSO-*d*₆. The successful synthesis of partially hydrolyzed PEO-*b*-P(AA-*stat*-*t*BA) copolymers with various degrees of polymerization was further verified by their different peak areas of the ^1H NMR spectra in DMSO-*d*₆ and CH₃OH-*d*₄. The -COOH signal did not appear in CH₃OH-*d*₄ because of proton exchange between the -COOH group of PAA and the -OD group of CH₃OH-*d*₄.

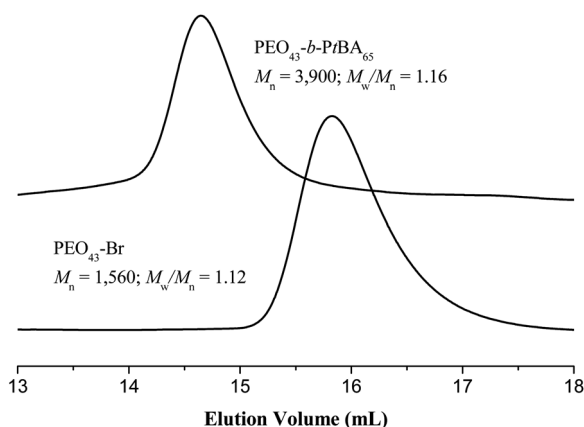


Fig. 2 GPC traces of PEO₄₃-*b*-PtBA₆₅ diblock copolymer and the PEO₄₃-Br macroinitiator, indicating the obvious chain extension of the PEO₄₃-*b*-PtBA₆₅ diblock copolymer compared with PEO₄₃-Br macroinitiator.

hydrolysis of the *Pt*BA in PEO-*b*-*Pt*BA diblock copolymer. By controlling the reaction time and the molar ratio of trifluoroacetic acid (TFA) to the ester groups, a series of PEO-*b*-P(AA-*stat*-*t*BA) block-statistical copolymers with various ratios of PAA to *Pt*BA were obtained, as shown in Table 1. The degrees of polymerization of PAA in polymers 2, 3 and 4 are 9, 25 and 50, respectively, according to the ^1H NMR analyses in Fig. 1.

Self-assembly of PEO-*b*-P(AA-*stat*-*t*BA) block-statistical copolymers

Three PEO-*b*-P(AA-*stat*-*t*BA) copolymers with different PAA and *Pt*BA compositions (polymers 2, 3 and 4 in Table 1) were self-assembled into vesicles in a mixture of THF-water

(1 : 2, v/v), with the P(AA-*stat*-*t*BA) chains forming the membrane, while the hydrophilic PEO chains being expressed at both the interior and exterior of the vesicle membrane. Transmission electron microscopy (TEM) study clearly confirmed the collapsed vesicular structure, as shown in Fig. 3. To improve the quality of TEM study, the vesicles from polymers 2 and 3 were stained by phosphotungstic acid (PTA), as shown in Fig. 3A and B, respectively. The corresponding number-averaged diameters of vesicles are ~ 189 and ~ 90 nm, respectively. The contours of larger vesicles became longer due to collapse of the soft vesicle membrane at high vacuum during TEM analysis.²³ The larger the vesicles were, the more likely they have collapsed. As demonstrated in Fig. 4A, dynamic laser light scattering (DLS) studies revealed that the mean intensity-averaged hydrodynamic diameter (D_h) of vesicles were in reasonably good agreement with TEM analysis. The correlation functions of the diluted aqueous vesicle solutions fit very well, as shown in Fig. 5.

Both DLS and TEM studies indicated that a higher ratio of PAA to *Pt*BA lead to larger vesicles and higher PDI. For example, at pH 6.0, the D_h values of the vesicles from polymers 2, 3 and 4 are 110, 175 and 272 nm, with PDIs of 0.015, 0.060 and 0.212, respectively, as shown in curves a to c in Fig. 6B. This is reasonable because the hydrophilic and pH-sensitive PAA chains were restrained in the vesicle membrane together with the hydrophobic *Pt*BA chains. To further test this hypothesis, the effect of solution pH on the size and PDI of the polymer vesicles was studied. Upon dialysis against water, the pH of the vesicle solution is 6.3. Then the pH value was tuned by aqueous HCl (pH 3) or NaOH (pH 12) solution. As expected, the D_h s of vesicles made from polymer 3 without crosslinking at pH 4.5,

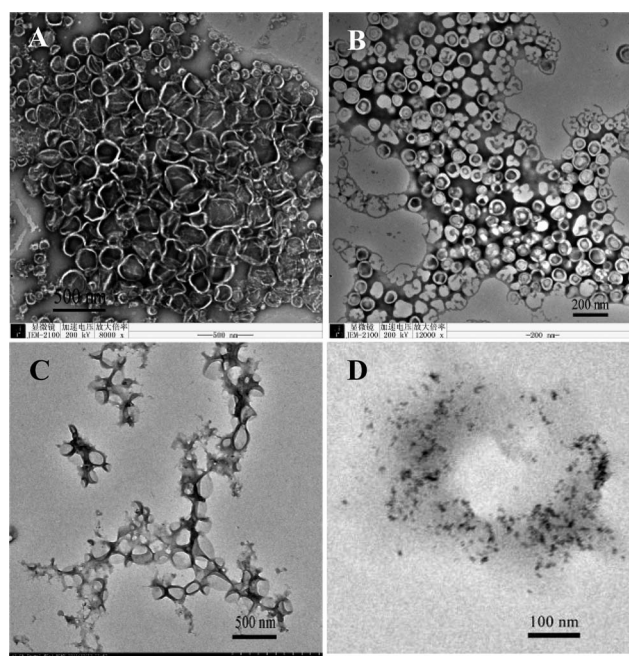


Fig. 3 TEM images of vesicles prepared using (A) polymer 3, (B) polymer 2 at an initial copolymer concentration (C_{ini}) of (A) 2.7 mg mL⁻¹ and (B) 5.0 mg mL⁻¹ in THF-water (1 : 2, v/v). The vesicles were stained by phosphotungstic acid for TEM analysis. (C) and (D): TEM images of magnetic vesicles prepared by *in situ* precipitating Fe₃O₄ nanoparticles in the membrane of polymer 3 vesicles at a C_{ini} of 2.0 mg mL⁻¹.

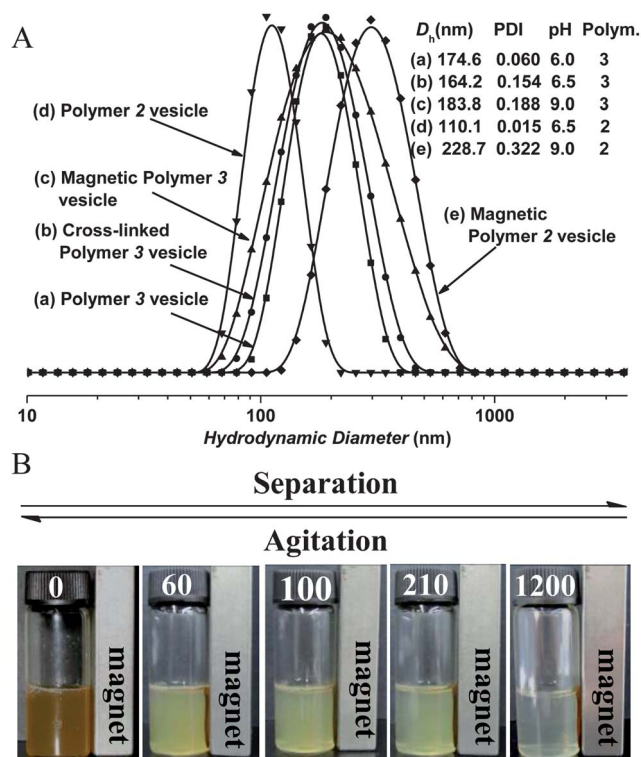


Fig. 4 (A) Intensity-averaged size distribution of vesicles prepared from polymer 3 (curves a–c) and polymer 2 (curves d and e) at various pH values and concentrations: (a) uncrosslinked vesicles at pH 6.0 and 0.27 mg mL^{-1} ; (b) crosslinked vesicles at pH 6.5 and 0.13 mg mL^{-1} ; (c) Fe_3O_4 -decorated magnetic vesicles at pH 9.0 and 0.1 mg mL^{-1} ; (d) uncrosslinked vesicles at pH 6.5 and 0.25 mg mL^{-1} ; (e) Fe_3O_4 -decorated superparamagnetic vesicles at pH 9.0 and 0.1 mg mL^{-1} . The size is determined by DLS. (B) A macroscopic view of Fe_3O_4 -decorated superparamagnetic polymer vesicles from 0–1200 min in an external magnetic field.

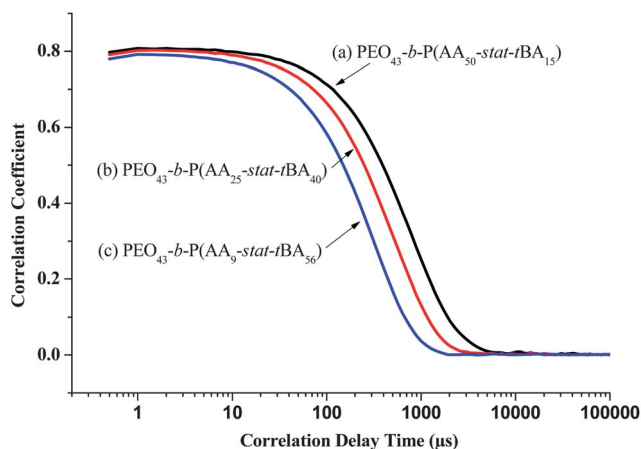


Fig. 5 Correlation functions of DLS studies of uncrosslinked polymer vesicles prepared from $\text{PEO}_{43}\text{-}b\text{-P}(\text{AA}\text{-}stat\text{-}t\text{BA})_{65}$ with various degrees of polymerization.

6.3 and 7.3 were 181, 177 and 233 nm, with PDIs of 0.085, 0.120 and 0.469, respectively (see Fig. 6A). The hypothesis was further verified by the correlation functions of the vesicle solutions at various pH in Fig. S2 (ESI[†]).

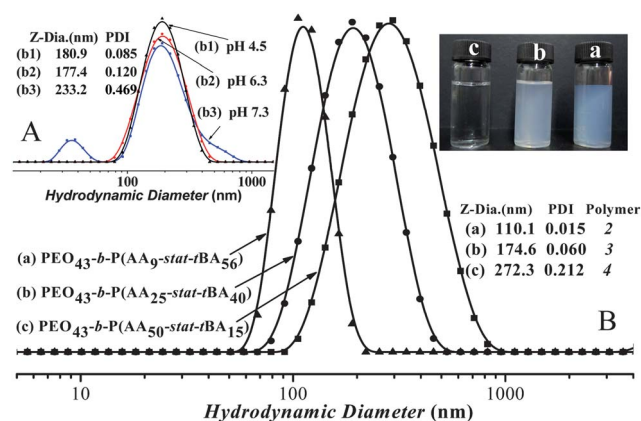


Fig. 6 (A) Intensity-averaged size distribution of $\text{PEO}_{43}\text{-}b\text{-P}(\text{AA}_{25}\text{-}stat\text{-}t\text{BA}_{40})$ (polymer 3) vesicles determined by DLS at 0.27 mg mL^{-1} at various pH conditions. (B) Intensity-averaged size distribution and digital photo of polymer vesicles prepared at pH 6 from (a) polymer 2 at an initial copolymer concentration ($C_{\text{ini}} = 1.8 \text{ mg mL}^{-1}$); (b) polymer 3 at $C_{\text{ini}} = 2.0 \text{ mg mL}^{-1}$; (c) polymer 4 at $C_{\text{ini}} = 0.75 \text{ mg mL}^{-1}$. The sizes were determined by DLS at $25 \text{ }^\circ\text{C}$.

Once the aqueous NaOH solution at pH 12 was added into the uncrosslinked vesicle solution, the PAA unit turned to be more hydrophilic because of the deprotonation of carboxylic groups, leading to the breaking of the vesicle membrane formed by $\text{P}(\text{AA}_{25}\text{-}stat\text{-}t\text{BA}_{40})$. The vesicles at pH > 7 may burst to reform smaller nanoparticles at $\sim 40 \text{ nm}$ (shown in curve b3 in Fig. 6A). This indicates that the higher PAA proportion and higher pH value lead to larger diameter and PDI of the vesicles. Also, to increase the colloidal stability of polymer vesicles at physiological conditions, it is essential to crosslink the vesicle membrane.

Selective crosslinking of partial PAA chains in the vesicle membrane

To obtain excellent *in vivo* stability, the vesicle membrane was partially crosslinked by selectively crosslinking the PAA *via* condensation reactions between the carboxylic groups of PAA and the amine functional groups of the crosslinker 2,2'-(ethylenedioxy)bis(ethylamine) in the presence of 1-(3-dimethylaminopropyl)-3-ethylcarbodiimide methiodide as the coupling reagent.³⁶ Scheme 1 illustrates the structure of the crosslinked vesicles: the random PAA-*stat*-PtBA chains form the compact vesicle membrane (the yellow and blue part), whereas the hydrophilic PEO chains form solvated vesicle coronas (the purple part) expressed inwards and outwards from the membrane. The average hydrodynamic diameter (by intensity) of polymer 3 vesicles with 20% crosslinking degree was smaller (164.2 nm) with a higher PDI (0.154), compared with uncrosslinked polymer 3 vesicles (174.6 nm, 0.060), as shown in curves a and b in Fig. 4A. The above results are consistent with the restricted state of PAA chains in the crosslinked vesicle membrane.

Deposition of superparamagnetic Fe_3O_4 nanoparticles

The superparamagnetic polymer vesicles were prepared by *in situ* chemical nanoprecipitation of iron oxides in the membrane of

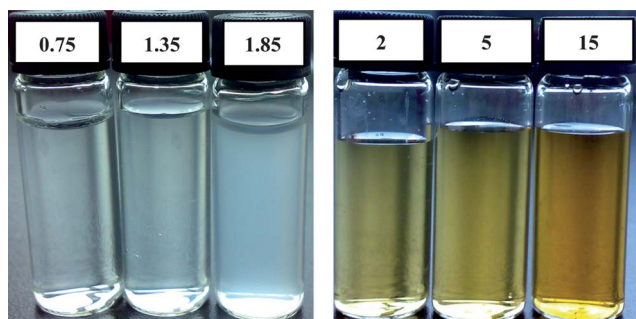


Fig. 7 Digital photos of PEO₄₃-*b*-(PAA₅₀-*stat*-PtBA₁₅) (polymer **4**) vesicles before and after *in situ* nanoprecipitation of superparamagnetic Fe₃O₄ at various concentrations. The concentrations of polymer vesicles before Fe₃O₄ deposition are 0.75, 1.35 and 1.85 mg mL⁻¹, as indicated on the labels. After Fe₃O₄ deposition: the magnetic vesicles prepared with increasing weight ratios of iron oxides (Fe₃O₄) relative to copolymer: 2, 5 and 15 wt%, from left to right.

the vesicles. A appropriate ratio of Fe³⁺/Fe²⁺ concentrations was designed to interact with carboxylate anions in PAA in the vesicle membrane. The Fe₃O₄ nanoparticles were precipitated *in situ* in the membrane of the vesicles by treating iron ions with aqueous NaOH solution. The solution immediately turned yellow and it gradually turned from yellow to brown after stirring at 60 °C for 2 h, indicating the resulting magnetic polymer vesicle formation. Fig. 7 shows the vesicle solutions with various concentrations before and after Fe₃O₄ nanoparticle deposition. Generally, the ratio of Fe³⁺/Fe²⁺ ions for preparation of Fe₃O₄ nanoparticles is 2/1. The average molar percentages of the carboxylic acid groups on vesicles we prepared are estimated at about 8, 23 and 46%, due to the increasing DP of AA unit in polymers **2**, **3** and **4**.

The molar ratio of Fe³⁺/COO⁻ affected the magnetism of the final magnetic vesicles. When the molar ratio of Fe³⁺/COO⁻ was fixed to 1/4.7, polymer vesicles possessed nearly the strongest magnetism.³⁷ As Fe³⁺ has a much higher affinity than Fe²⁺ for carboxylic groups,³⁸ we adopted the molar ratio of Fe³⁺/COO⁻ as 1/4.7, with an excess of Fe²⁺ (the mole ratio of Fe³⁺ to Fe²⁺ was 1/3).

DLS and TEM studies of superparamagnetic vesicles

DLS and TEM studies were conducted to reveal the morphology and the size of the superparamagnetic vesicles. Fig. 4A shows the DLS studies on the uncrosslinked vesicles, vesicles with 20% crosslinking degree, and superparamagnetic vesicles prepared from polymers **2** and **3**. The hydrodynamic diameters (*D_h*) of the three types of vesicles prepared from polymer **3** were 174.6, 164.2 and 183.8 nm with the polydispersity increased slightly from 0.060 to 0.154 and then 0.188. Moreover, the superparamagnetic vesicles can move regularly and congregate under the exertion of an external magnet, as shown in Fig. 4B. After 1200 min, the superparamagnetic polymer vesicles totally congregate while they can be easily redispersed after agitation for many cycles.

As shown in Fig. 3C and D, TEM study confirmed successful *in situ* precipitation of Fe₃O₄ nanoparticles within the membrane of the polymer vesicles. The size of the Fe₃O₄ nanoparticles was estimated as ~6 nm with a narrow distribution, which is consistent with their superparamagnetic behaviour (usually <10 nm).

TGA of superparamagnetic vesicles

To attempt to reveal the content of iron oxide in the superparamagnetic polymer vesicles, TGA studies of the Fe₃O₄-decorated polymer vesicle powder prepared from polymers **2** and **3** were carried out in a nitrogen atmosphere. As shown in Fig. S3 (ESI[†]), at temperatures below 100 °C a small weight loss was attributed to the vaporization of residual or absorbed solvent. Then two stages of large weight loss occurred around 250 and 420 °C, indicating the decomposition and gasification of water and the high-molecular-weight polymer. The small weight loss at 600 °C might be attributed to the breakdown of the COO⁻ group coordinated with Fe₃O₄ nanoparticles in the magnetic vesicles. There was nearly no weight loss occurring after 750 °C with residual mass percentages of 5% (polymer **2**, Fig. S3A, ESI[†]) and 20% (polymer **3**, Fig. S3B, ESI[†]), which were higher than the theoretical Fe₃O₄ contents (2 and 4%), indicating the incomplete gasification of the organic materials during TGA.³⁹

Iron titration

To further titrate the iron oxide in the magnetic polymer vesicles, the total iron concentrations of magnetic vesicles of polymers **2** and **3** were determined by atomic absorption spectroscopy (AAS) as 0.62 and 1.24 mmol L⁻¹, which were slightly higher than the theoretical value of 0.52 and 1.04 mmol L⁻¹, possibly because partial excess Fe²⁺ was oxidized to Fe³⁺.

Magnetic hysteresis loops of superparamagnetic vesicles

The magnetic hysteresis loops determined by SQUID in the field *H* range of ±5000 Oe at 300 K shown in Fig. S4 (ESI[†]) proved the superparamagnetic behaviour of the polymer vesicles decorated with iron oxide. The specific saturation magnetization (*M_s*) was 3.2 emu g⁻¹, which was much smaller than for pure Fe₃O₄. The decrease in the value of *M_s* could be attributed to the rather smaller size of the Fe₃O₄ nanoparticles and the relatively low amount of Fe₃O₄ loaded in the vesicles,⁴⁰ which was estimated at 4.8 wt% according to the content of Fe determined by atomic absorption spectroscopy. Fig. S4 (ESI[†]) also indicated that the polymer vesicles showed superparamagnetic behavior with almost no remanence and coercivity at room temperature.

Zeta potential of polymer vesicles

As shown in Table 2, the zeta potentials (*ζ*) of vesicles prepared from polymers **2** and **3** without crosslinking or decoration of Fe₃O₄ nanoparticles in the vesicle membrane were -20.4 mV at pH 6.5 and -26.3 mV at pH 6.0 (just after dialysis, without pH tuning), respectively. When the pH was increased to the physiological value of 7.4, the zeta potentials became -24.0 and -36.0 mV, indicating more deprotonated carboxylic acid groups. In both cases, polymer **3** vesicles have more negative charges due to more carboxylic acid groups compared with polymer **2** vesicles. The zeta potential of the vesicles prepared from polymers **2** and **3** (20% crosslinking degree) and decorated with superparamagnetic Fe₃O₄ nanoparticles became -14.2 mV at pH 6.5 and -9.67 mV at pH 6.0 due to the interactions between Fe³⁺/Fe²⁺ and carboxylate anions in the vesicle membrane.

Table 2 Zeta potentials of vesicles with and without Fe₃O₄ nanoparticles

Polymer	Composition	ζ_1^a /mV	ζ_2^b /mV	ζ_3^c /mV
2	PEO ₄₃ - <i>b</i> -P(AA ₉ - <i>stat</i> - <i>t</i> BA ₅₆)	-20.4	-24.0	-14.2
3	PEO ₄₃ - <i>b</i> -P(AA ₂₅ - <i>stat</i> - <i>t</i> BA ₄₀)	-26.3	-36.0	-9.67

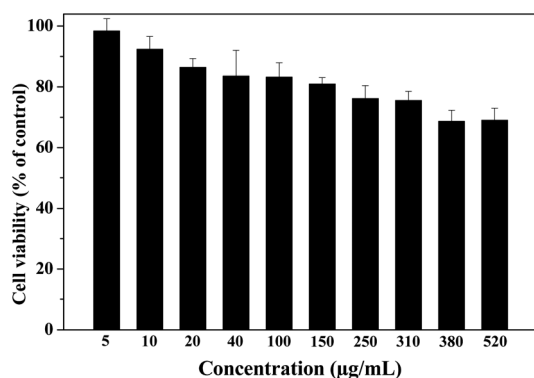
^a Zeta potentials (ζ_1) of polymer vesicles at pH 6.5 (polymer 2) and 6.0 (polymer 3) after dialysis without Fe₃O₄. ^b Zeta potentials (ζ_2) of vesicles without Fe₃O₄ at pH 7.4. ^c Zeta potentials (ζ_3) of vesicles with superparamagnetic Fe₃O₄ nanoparticles at pH 6.5 (polymer 2) and 6.0 (polymer 3).

Cytotoxicity study

The cytotoxicity of the Fe₃O₄-decorated polymer 3 magnetic vesicles against HeLa cells was carried out by using a MTT (3-(4,5-dimethylthiazol-2-yl)-2,5-diphenyltetrazolium bromide) assay. HeLa cells were treated with the magnetic polymer 3 vesicles at various concentrations. As shown in Fig. 8, the cell viability was calculated using the ratio of the number of HeLa cells of the treated group over the untreated control. This demonstrated that Fe₃O₄-decorated magnetic vesicles from PEO₄₃-*b*-P(AA₂₅-*stat*-*t*BA₄₀) copolymer did not significantly affect the cell viability and proliferation of HeLa cells at various concentrations $\leq 520 \mu\text{g mL}^{-1}$. The IC₅₀ of the superparamagnetic vesicles on HeLa cells is $782 \mu\text{g mL}^{-1}$. The cell viabilities at magnetic vesicle concentrations of 100 and $150 \mu\text{g mL}^{-1}$ (equivalent to Fe concentration 65 and $97 \mu\text{M}$) were nearly 90%, which were good enough to meet the concentration requirement of Fe₃O₄ in MR imaging application.

MR imaging

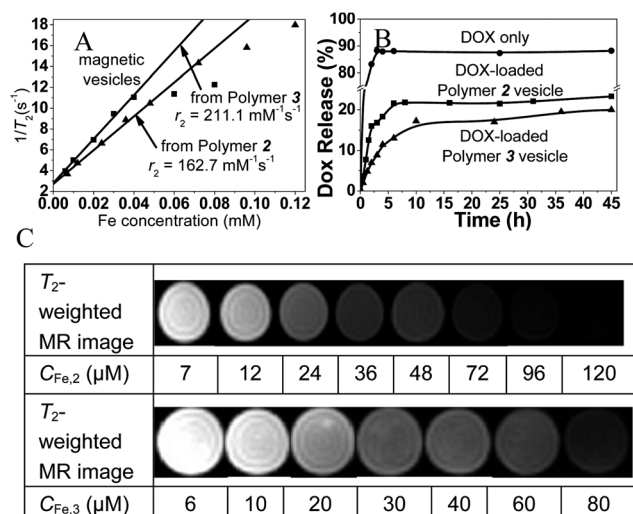
In general, the efficiency of an MRI contrast agent based on SPIONs is assessed by calculating its longitudinal and transverse relaxivities, r_1 and r_2 , which reflect the ability of the contrast agent to T_1 (spin-lattice relaxation) and T_2 (spin-spin relaxation), respectively.³⁴ Relaxivities can be calculated through the linear least-squares fitting of $1/\text{relaxation time (s}^{-1})$ vs. the iron concentration (mM, Fe).³⁵ In the previous reports, SPIO nanoparticles are present as clusters inside micelle cores or vesicle cavities, and the T_2 relaxivity (r_2) can be considerably increased due to the short distance of nanoparticle assemblies.^{34,35,41,42} In our study, water-dispersible SPIONs were distributed within the

**Fig. 8** Cell proliferation of HeLa cells after 24 h incubation with Fe₃O₄-decorated polymer 3 magnetic vesicles.

membrane of the polymer vesicles, and the relaxation times were measured at 3 T on a Siemens MRI scanner at room temperature. SPIONs are generally used as T_2 contrast agents. Fig. 9A shows the measurement of the r_2 relaxivity for the Fe₃O₄-decorated magnetic vesicles. The r_2 of the magnetic vesicles prepared from polymers 2 and 3 were 162.7 and $211.1 \text{ mM}^{-1} \text{ s}^{-1}$, while the reported r_2 value of a commercially available SPIO-based MRI contrast agent, Feridex, was $105 \text{ mM}^{-1} \text{ s}^{-1}$.⁴³ As a result of the interference of noise, the T_2 relaxation rate ($1/T_2$) at $C_{\text{Fe}} \geq 80 \mu\text{M}$ was lower than the theoretical value. To further evaluate the detection sensitivity of the Fe₃O₄-decorated magnetic vesicles, typical T_2 -weighted spin-echo images recorded for magnetic vesicles from polymers 2 and 3 at a superparamagnetic Fe₃O₄ nanoparticle loading content of 2.4 and 4.8 wt% are shown in Fig. 9C. T_2 -weighted images of the vesicles at various Fe concentrations were also collected at 3 T (spin-echo sequence, $T_R = 8000 \text{ ms}$, $T_E = 13.6 \text{ ms}$, room temperature). This confirms that the water-dispersible Fe₃O₄-decorated magnetic polymer vesicles can serve as a highly efficient T_2 contrast agent.

Drug release of DOX-loaded vesicles

DOX is a water-soluble anticancer drug in its hydrochloride salt form. DOX release profiles in Fig. 9B obtained for a control experiment utilizing an aqueous solution of 0.050 mg mL^{-1} DOX in the absence of any vesicles indicated rapid drug release (circles), as expected. In contrast, an aqueous solution of DOX-loaded vesicles prepared by dissolving DOX·HCl with polymer 2 or polymer 3 in THF-water, followed by dialysis against deionized water to remove free drug, produced a much slower drug release profile (squares and triangles). For these latter DOX-loaded vesicles, the DOX concentration was 0.690 mg mL^{-1} after subsequent dialysis against pH 7.4 tris buffer for 45 h, and the drug loading efficiency is estimated to be

**Fig. 9** (A) T_2 relaxation rate ($1/T_2$) as a function of iron concentration recorded for aqueous solutions (25°C) of magnetic vesicles prepared from polymers 2 and 3 and decorated with ~ 2.4 and ~ 4.8 wt% superparamagnetic Fe₃O₄ nanoparticles, respectively. (B) DOX release profiles of vesicles from polymers 2 and 3 in 0.01 M tris buffer at pH 7.4 and 37°C . (C) T_2 -weighted MR images obtained from magnetic vesicles prepared from polymer 2 (top) and polymer 3 (bottom).

approximately 22.5% (vesicles from polymer **2**) and 26.9% (vesicles from polymer **3**). It is well-established that hydrophilic anticancer drugs such as DOX·HCl can be physically encapsulated within the vesicle cavities, and the release profile indicates significantly retarded release of the drug at pH 7.4 due to its entrapment within the vesicles.

Experimental section

Materials and methods

Poly(ethylene oxide) methyl ether (MeO-PEO-OH; $M_n = 1900$) was purchased from Alfa Aesar and dried azeotropically with toluene to remove traces of water. Triethylamine (TEA) was dried by refluxing over CaH₂ and distilled prior to use. *tert*-Butyl acrylate (*t*BA; purchased from Tokyo Chemical Industry Co., Ltd.) monomer was purified through a silica column to remove inhibitor before use. *N,N,N',N'',N'''*-Pentamethyldiethylenetriamine (PMDETA; 98%) and 2-bromoisobutyl bromide were obtained from Aladdin Chemistry, Co. (Shanghai, China). 2,2'-(Ethylenedioxy)bis(ethylamine) and 1-(3-dimethylaminopropyl)-3-ethylcarbodiimide methiodide were purchased from Aldrich and used as received. Trifluoroacetic acid (TFA), FeCl₃·6H₂O, FeCl₂·4H₂O, CuBr, THF, dichloromethane (DCM) and other reagents were purchased from Sinopharm Chemical Reagent Co., Ltd. (SCRC, Shanghai, China) and used as received.

Synthesis of PEO-Br macro-initiator

The preparation of PEO-Br macro-initiator was carried out by the esterification between MeO-PEO-OH and 2-bromoisobutyl bromide. First, MeO-PEO-OH (10.00 g, 0.0053 mol) was dissolved in 250 mL toluene in a 500 mL round-bottom flask at 130 °C to remove traces of water by azeotropic distillation. After cooling down the solution to room temperature, distilled anhydrous triethylamine (1.90 mL, 13.2 mmol) was added into the flask with a syringe, followed by adding 2-bromoisobutyl bromide (1.66 mL, 13.2 mmol; dissolved in 20 mL anhydrous toluene) dropwise over 1 h. After stirring in an ice–water bath for 48 h, the solution was filtered to remove the produced triethylamine hydrobromide and the solvent was removed by rotary evaporation. The crude product was dissolved in dichloromethane (DCM; 50 mL) and washed with deionized water (50 mL), the organic phase was collected and the water phase was extracted twice using DCM. Then all the obtained organic phase was washed by 1.0 M HCl and 1.0 M NaOH solutions, and dried over anhydrous MgSO₄ overnight. After the solution was concentrated with rotary evaporation, the by-products and impurities were removed by precipitation in 300 mL diethyl ether three times. The product was dried under vacuum for 24 h. Yield: ~80%.

Synthesis of PEO-*b*-PtBA diblock copolymer

A round-bottom flask charged with CuBr (0.1080 g, 0.0007 mol) and PEO₄₃-Br macro-initiator (1.500 g, 0.0007 mol) was degassed by freeze–pump–thaw cycles three times to remove any oxygen. Deoxygenated *t*BA (7.600 g, 0.0593 mol), PMDETA (0.1290 g, 0.0007 mol) and anhydrous methanol (15 mL) were then added into the flask *via* a gas-tight syringe. The flask was placed in an oil-bath at 60 °C and stirred for 48 h. After removal

of methanol by rotary evaporation, DCM was added into the flask to dissolve the polymer. The mixture was then filtered through a silica column to remove the copper. The polymer solution was concentrated by rotary evaporation. For further purification, the desired copolymer was dissolved in THF, transferred into a dialysis tube, and dialyzed against deionized water for 2 days to remove traces of residual *t*BA monomer. A white powder was obtained after lyophilization.

Synthesis of PEO-*b*-P(AA-*stat*-*t*BA) diblock copolymer

PEO-*b*-P(AA-*stat*-*t*BA) was prepared by partial hydrolysis of PEO-*b*-PtBA diblock copolymer. Briefly, PEO-*b*-PtBA (2.000 g, 0.2 mmol) was dissolved in 10 mL DCM in a round-bottom flask, followed by trifluoroacetic acid at various TFA : *t*BA molar ratios (ranging from 1 : 1 to 5 : 1), and the mixture was allowed to stir at room temperature. The solvent and excess TFA were removed by rotary evaporation. Then the light yellow polymer solid was dried under vacuum for 2 days. The sticky light yellow solid was purified by exhaustive dialysis against deionized water for 2 days. After lyophilization a white powder of PEO-*b*-P(AA-*stat*-*t*BA) was obtained.

Self-assembly of copolymer into vesicles

To prepare the copolymer vesicles, PEO-*b*-P(AA-*stat*-*t*BA) (30 mg) was dissolved in 3.0 mL THF and 6.0 mL deionized water was added dropwise to the copolymer solution in 30 min by a gas-tight syringe with continuous stirring. Then the solution was transferred into a dialysis tube to dialyze against deionized water for 3 days by changing water twice each day to remove THF.

Selectively crosslinking the PAA blocks in the vesicles

The catalyst 1-(3-dimethylaminopropyl)-3-ethylcarbodiimide methiodide was added dropwise to the aqueous PEO-*b*-P(AA-*stat*-*t*BA) block copolymer vesicle solution. After stirring for 10 min, the crosslinker, 2,2'-(ethylenedioxy)bis(ethylamine), was added dropwise into the solution. The reaction mixture was allowed to stir overnight at room temperature and then dialyzed against deionized water for 3 days to remove byproducts during the crosslinking reaction.³⁶

Preparation of superparamagnetic polymer vesicles

The magnetic vesicles were prepared by chemical precipitation of Fe₃O₄ within the membrane of the block copolymer vesicles. The pH of the diluted crosslinked vesicle solutions prepared from PEO-*b*-P(AA-*stat*-*t*BA) diblock copolymer was tuned to 7 by aqueous NaOH solution (0.01 M) to transform the carboxylic acid groups to carboxylate anions. The flask was then purged with argon for 30 min. An aqueous FeCl₃·6H₂O and FeCl₂·4H₂O solution was also purged with argon for 30 min and then added to the flask. The mixture was stirred overnight for ion exchange under argon protection. An aqueous NaOH solution (0.1 M) was then added dropwise under argon at 30 °C and the mixture was stirred at 60 °C for 2 h.

Characterization

The molecular weight of the PEO-*b*-P7BA diblock copolymer and the PEO-Br macro-initiator were assessed by gel permeation chromatography (GPC) which was carried out with a Waters Breeze 1525 GPC analysis system with two PL mix-D columns using poly(ethylene oxide) (PEO, purchased from TOSOH) as standard. The mobile phase was DMF with 0.5 M LiBr at a flow rate of 1.0 mL min⁻¹ and 80 °C.

Proton nuclear magnetic resonance (¹H NMR) spectra were recorded using Bruker AV 400 MHz spectrometers, with CDCl₃, CD₃OD and DMSO-*d*₆ as solvents and TMS as standard at room temperature.

DLS studies of aqueous polymer vesicle and magnetic vesicle solutions were determined using Nano-ZS 90 Nanosizer (Malvern Instruments Ltd., Worcestershire, UK) at a fixed scattering angle of 90°. The data were processed by cumulative analysis of the experimental correlation function, and particle diameters were calculated from the computed diffusion coefficients using the Stokes–Einstein equation. Each reported measurement was conducted for three runs.

Zeta potential studies of aqueous polymer vesicle solution with and without superparamagnetic Fe₃O₄ nanoparticles were determined using a Nano-ZS 90 Nanosizer (Malvern Instruments Ltd., Worcestershire, UK) at various pH. No background electrolyte was added. Each reported measurement was conducted for three runs.

TEM images were obtained using a JEM-2100 electron microscope operating at an acceleration voltage of 200 kV. To prepare TEM samples, 5 μL of diluted vesicles or magnetic vesicle suspension was dropped onto a carbon-coated copper grid and the former was negatively stained with 1% phosphotungstic acid (pH = 5–6). The water droplet was allowed to evaporate slowly under ambient conditions before measurement. Magnetic vesicles were not stained by any staining agent.

Thermogravimetric analysis (TGA) experiments were conducted using a Perkin Elmer thermal gravimetric and differential thermal analysis instrument (America) from room temperature to 1000 °C with a heating rate of 10 °C min⁻¹ in N₂ flow.

The magnetization curve of the magnetic vesicles was measured as a function of the applied magnetic field *H* with a 9600 VSM (LDJ Co.) superconducting quantum interference device (SQUID) magnetometer. The hysteresis of the magnetization was obtained by varying *H* between +5000 and –5000 Oe at 300 K.

In ion titration measurements the total iron concentration (mol L⁻¹) was determined by TAS-990 atomic absorption spectroscopy (AAS) after degrading the Fe₃O₄-decorated vesicles in boiling HCl (35%).

UV-vis studies were conducted using an UV-vis spectrophotometer (UV-759S, Q/YXL270, SHANGHAI PRECISION & SCIENTIFIC INSTRUMENT CO., Ltd) with a scan speed of 300 nm min⁻¹. The absorbance and transmittance spectra of the hybrid vesicles were recorded in the range of 300–650 nm.

Cytotoxicity test

The cytotoxicity of the magnetic polymer vesicles against HeLa cells was evaluated by measuring the inhibition of cell growth

using the MTT assay. First, HeLa cells were seeded in a 96-well plate at a density of 5000 cells per well and incubated overnight at 37 °C in a humidified 5% CO₂ atmosphere using Deulbecco's Modified Eagle Medium (DMEM). Subsequently, the cells were incubated with various concentrations of magnetic vesicles ranging from 5 to 520 μg mL⁻¹ for 24 h. Thereafter, the cell culture medium in each well was replaced with 100 μL fresh media and the HeLa cells were incubated again for another 3 h with 20 μL of 5 mg mL⁻¹ sterile filtered 3-(4,5-dimethylthiazol-2-yl)-2,5-diphenyltetrazolium bromide (MTT) in warm PBS. After removing the culture medium, 100 μL of DMSO was added into each well and the plate was incubated at room temperature for 10 min on a shaking platform. The resulting solution was measured for absorbance at 570 nm using a Multiscan MK3 plate reader. The cell viability was obtained by calculation according to the ratio of the intensity of purple formazan in viable cells treated with magnetic vesicles to the intensity in untreated control cells.

DOX loading and *in vitro* release

PEO₄₃-*b*-P(AA₉-*stat*-tBA₅₆) diblock copolymer (10.0 mg) and anticancer drug DOX·HCl (4.0 mg) were dissolved in THF (2.0 mL), and 4.0 mL deionized water was added dropwise to the solution over a 30 min period by a gas-tight syringe with continuous stirring. DOX-loaded vesicles were formed by dialysis against 500 mL deionized water at 20 °C for 4 h.⁴⁴ The dialysis medium was changed every 0.5 h and the whole procedure was performed in the dark. The drug loading efficiency in the dialyzed vesicle solution was determined using a UV-vis spectrophotometer (UV-759S, Q/YXL270) to compare the absorbance of this solution at 483 nm with a calibration curve of aqueous DOX solutions with known concentration.

To investigate the *in vitro* release profile, the DOX-vesicle mixture was subsequently dialyzed against 50 mL of a 0.01 M tris buffer at pH 7.4 and 37 °C for 45 h prior to an elution experiment. At desired time intervals, 3.0 mL release media was taken out to determine the DOX concentration at 483 nm by using fluorescence measurement, then added into the release system after measurement.

The drug loading efficiency and the cumulative DOX release were calculated according to the following formulae:⁴⁵

$$\text{Drug loading efficiency (wt\%)} = (M_0/M_a) \times 100\%$$

$$\text{Cumulative DOX release (\%)} = (M_t/M_0) \times 100\%$$

where *M_a* is the weight of total DOX added, *M_t* is the total amount of DOX released from vesicles at time *t*, and *M₀* is the amount of DOX initially loaded into the vesicles.

A control solution without any polymer was prepared by simply adding 0.9 mg DOX to 10.0 mL of water in the dialysis tubing. This sample was not dialyzed prior to elution. The elution experiments were carried out immediately after the DOX-vesicle samples were dialyzed. The DOX solution was added to the dialysis tubing and dialyzed against 50 mL of 0.01 M tris buffer at pH 7.4 and 37 °C. After suitable time intervals, 3.0 mL of tris buffer solution was periodically removed to determine the DOX concentration at 483 nm by UV-vis measurement.²²

MR imaging

The T_2 weights of the magnetic vesicle solution at various concentrations were measured with a Siemens Trio 3 T clinical MRI instrument at room temperature. The transverse T_2 measurements were acquired using a multiple spin-echo 2D imaging sequence ($T_R = 8000$ ms, $T_E = 13.6$ ms (10 echoes), $SL = 2$ mm, $FOV = 60 \times 60$ mm, $MA = 128 \times 128$). Relaxation times were obtained by fitting the multi-echo data to a monoexponential decay curve using linearized least-squares optimization. Relaxivity values were calculated *via* linear least-squares fitting of $1/T_2$ relaxation time (s^{-1}) vs. the iron concentration (mM Fe).

Conclusions

In summary, a novel class of multifunctional polymer vesicles was prepared by self-assembly of a new class of amphiphilic PEO₄₃-*b*-P(AA_{*x*}-*stat*-tBA_{65-*x*}) copolymers in aqueous solution. DLS studies confirmed the vesicle formation and their excellent water dispersibility and colloidal stability in aqueous solution. TEM studies revealed the vesicle morphology and the ultrafine Fe₃O₄ nanoparticles (~6 nm) engineered within the membrane of the polymer vesicles by *in situ* chemical nanoprecipitation, leading to a very low specific saturation magnetization and an ultra-high T_2 relaxivity (211.1 mM⁻¹ s⁻¹). The low iron content leads to a weak coalescence in a strong magnetic field. The partial crosslinking of the vesicle membrane offers the superparamagnetic vesicles excellent colloidal stability at a wide range of pH conditions. The *in vitro* studies showed that the superparamagnetic polymer vesicles had excellent biocompatibility and ultrasensitivity as a MR imaging contrast agent. Moreover, the anti-tumour drug release experiment revealed that the polymer vesicles can be employed for drug delivery. Thus, these multifunctional polymer vesicles decorated with superparamagnetic Fe₃O₄ nanoparticles are promising candidates for cancer theranostics and nanomedicine.

Acknowledgements

J. D. is supported by the CXY project and the Key Project of Innovative Scientific Research of Shanghai Education Commission (11CXY16 and 11ZZ31), Pujiang Project of Shanghai Science and Technology Commission (10PJ1409900), National Natural Science Foundation of China (21074095 and 21174107), Fok Ying Tong Education Foundation (132018), the Program for Professor of Special Appointment (Eastern Scholar) at Shanghai Institutions of Higher Learning, Shanghai 1000 Plan, the Fundamental Research Funds for the Central Universities (0500219141), New Century Excellent Talents in Universities of Ministry of Education (NCET-10-0627), PhD Program Foundation of Ministry of Education (20110072110048), SRF for ROCS, SEM and the Startup Package of Tongji University.

Notes and references

- 1 WHO, *World Health Statistics*, Geneva, 2008.
- 2 M. D. Pegram, G. E. Konecny, C. O'Callaghan, M. Beryt, R. Pietras and D. J. Slamon, *J. Natl. Cancer Inst.*, 2004, **96**, 739–749.
- 3 S. M. Janib, A. S. Moses and J. A. MacKay, *Adv. Drug Delivery Rev.*, 2010, **62**, 1052–1063.

- 4 C. Sun, J. S. H. Lee and M. Q. Zhang, *Adv. Drug Delivery Rev.*, 2008, **60**, 1252–1265.
- 5 M. E. Davis, Z. Chen and D. M. Shin, *Nat. Rev. Drug Discovery*, 2008, **7**, 771–782.
- 6 R. R. Qiao, C. H. Yang and M. Y. Gao, *J. Mater. Chem.*, 2009, **19**, 6274–6293.
- 7 J. Qin, S. Laurent, Y. S. Jo, A. Roch, M. Mikhaylova, Z. M. Bhujwala, R. N. Muller and M. Muhammed, *Adv. Mater.*, 2007, **19**, 1874–1878.
- 8 A. K. Gupta and M. Gupta, *Biomaterials*, 2005, **26**, 3995–4021.
- 9 D. H. Carr, J. Brown, G. M. Bydder, H. J. Weinmann, U. Speck, D. J. Thomas and I. R. Young, *Lancet*, 1984, **323**, 484–486.
- 10 L. W. Liu, H. Ding, K. T. Yong, I. Roy, W. C. Law, A. Kopwithaya, R. Kumar, F. Erogbogbo, X. H. Zhang and P. N. Prasad, *Plasmonics*, 2010, **6**, 105–112.
- 11 A. Bianchi, L. Calabi, F. Corana, S. Fontana, P. Losi, A. Maiocchi, L. Paleari and B. Valtancoli, *Coord. Chem. Rev.*, 2000, **204**, 309–393.
- 12 A. H. Lu, E. L. Salabas and F. Schuth, *Angew. Chem., Int. Ed.*, 2007, **46**, 1222–1244.
- 13 S. Laurent, D. Forge, M. Port, A. Roch, C. Robic, L. V. Elst and R. N. Muller, *Chem. Rev.*, 2008, **108**, 2064–2110.
- 14 D. E. Discher and A. Eisenberg, *Science*, 2002, **297**, 967–973.
- 15 J. Z. Du and R. K. O'Reilly, *Soft Matter*, 2009, **5**, 3544–3561.
- 16 J. Z. Du, Y. M. Chen, Y. H. Zhang, C. C. Han, K. Fischer and M. Schmidt, *J. Am. Chem. Soc.*, 2003, **125**, 14710–14711.
- 17 S. F. M. van Dongen, H. P. M. de Hoog, R. J. R. W. Peters, M. Nallani, R. J. M. Nolte and J. C. M. van Hest, *Chem. Rev.*, 2009, **109**, 6212–6274.
- 18 D. J. Irvine, *Nat. Mater.*, 2011, **10**, 342–343.
- 19 J. Z. Du and R. K. O'Reilly, *Chem. Soc. Rev.*, 2011, **40**, 2402–2416.
- 20 M. A. C. Stuart, W. T. S. Huck, J. Genzer, M. Muller, C. Ober, M. Stamm, G. B. Sukhorukov, I. Szleifer, V. V. Tsukruk, M. Urban, F. Winnik, S. Zauscher, I. Luzinov and S. Minko, *Nat. Mater.*, 2010, **9**, 101–113.
- 21 J. Z. Du, H. Willcock, J. P. Patterson, I. Portman and R. K. O'Reilly, *Small*, 2011, **7**, 2070–2080.
- 22 J. Z. Du, Y. Q. Tang, A. L. Lewis and S. P. Armes, *J. Am. Chem. Soc.*, 2005, **127**, 17982–17983.
- 23 J. Z. Du and S. P. Armes, *J. Am. Chem. Soc.*, 2005, **127**, 12800–12801.
- 24 H. Ding, F. Wu, Y. Huang, Z. R. Zhang and Y. Nie, *Polymer*, 2006, **47**, 1575–1583.
- 25 S. H. Qin, Y. Geng, D. E. Discher and S. Yang, *Adv. Mater.*, 2006, **18**, 2905–2909.
- 26 Y. Zhao, *Chem. Rec.*, 2007, **7**, 286–294.
- 27 T. B. Ren, Y. Feng, Z. H. Zhang, L. Li and Y. Y. Li, *Soft Matter*, 2011, **7**, 2329–2331.
- 28 Q. Yan, J. Y. Yuan, Z. N. Cai, Y. Xin, Y. Kang and Y. W. Yin, *J. Am. Chem. Soc.*, 2010, **132**, 9268–9270.
- 29 J. K. Oh and J. M. Park, *Prog. Polym. Sci.*, 2011, **36**, 168–189.
- 30 S. H. Yuk, K. S. Oh, H. Koo, H. Jeon, K. Kim and I. C. Kwon, *Biomaterials*, 2011, **32**, 7924–7931.
- 31 K. Wang, H. Q. Dong, H. Y. Wen, M. Xu, C. Li, Y. Y. Li, H. N. Jones, D. L. Shi and X. Z. Zhang, *Macromol. Biosci.*, 2011, **11**, 65–71.
- 32 C. J. F. Rijcken, O. Soga, W. E. Hennink and C. F. van Nostrum, *J. Controlled Release*, 2007, **120**, 131–148.
- 33 C. Sanson, O. Diou, J. Thevenot, E. Ibarboure, A. Soum, A. Brulet, S. Miraux, E. Thiaudiere, S. Tan, A. Brisson, V. Dupuis, O. Sandre and S. Lecommandoux, *ACS Nano*, 2011, **5**, 1122–1140.
- 34 X. Q. Yang, J. J. Grailler, I. J. Rowland, A. Javadi, S. A. Hurley, V. Z. Matson, D. A. Steeber and S. Q. Gong, *ACS Nano*, 2010, **4**, 6805–6817.
- 35 X. Q. Yang, J. J. Grailler, I. J. Rowland, A. Javadi, S. A. Hurley, D. A. Steeber and S. Q. Gong, *Biomaterials*, 2010, **31**, 9065–9073.
- 36 Q. Zhang, E. E. Remsen and K. L. Wooley, *J. Am. Chem. Soc.*, 2000, **122**, 3642–3651.
- 37 J. S. Huang, S. R. Wan, M. Guo and H. S. Yan, *J. Mater. Chem.*, 2006, **16**, 4535–4541.
- 38 M. Zhang, B. Wang, Y. Zhang and B. He, *Ion Exch. Adsorption*, 1995, **11**, 302–308.
- 39 H. Shang, W. S. Chang, S. Kan, S. A. Majetich and G. U. Lee, *Langmuir*, 2006, **22**, 2516–2522.
- 40 X. Y. Yang, X. Y. Zhang, Y. F. Ma, Y. Huang, Y. S. Wang and Y. S. Chen, *J. Mater. Chem.*, 2009, **19**, 2710–2714.

-
- 41 M. Lattuada and T. A. Hatton, *J. Am. Chem. Soc.*, 2007, **129**, 12878–12889.
- 42 J. F. Berret, N. Schonbeck, F. Gazeau, D. El Kharrat, O. Sandre, A. Vacher and M. Airiau, *J. Am. Chem. Soc.*, 2006, **128**, 1755–1761.
- 43 M. Rohrer, H. Bauer, J. Mintorovitch, M. Requardt and H. J. Weinmann, *Invest. Radiol.*, 2005, **40**, 715–724.
- 44 L. Sun and J. Z. Du, *Polymer*, 2012, **53**, 2068–2073.
- 45 J. Z. Du, Y. Q. Tang, A. L. Lewis and S. P. Armes, *J. Controlled Release*, 2011, **152**, E16–E17.